

Structure of Arnold tongues and the $f(\alpha)$ spectrum for period doubling: Experimental results

James A. Glazier, Mogens H. Jensen, Albert Libchaber, and Joel Stavans
The James Franck Institute, The University of Chicago, Chicago, Illinois 60637
 (Received 24 April 1986)

We study experimentally the detailed structure of resonances in forced Rayleigh-Bénard convection in mercury. The resonances appear as Arnold tongues in the phase diagram of the system. We follow a particular tongue beyond the critical line where tongues start to overlap and find a period-doubling curve stretching over the entire tongue. Above this line there is a symmetry breaking with period-doubling cascades at the two sides of the tongue. We also observe a multitude of other periodic windows in this regime together with hysteresis effects caused by overlap of other tongues. We follow one of the period-doubling cascades and study the full scaling structure of the attractor at the onset of chaos by means of an $f(\alpha)$ spectrum of scaling indices. The experimental spectrum is, within error, the same as the universal spectrum calculated theoretically.

When an oscillating system with a characteristic frequency ω_{int} is perturbed by an external oscillation of frequency ω_{ext} , and the two oscillators couple nonlinearly, one observes resonances where the ratio $\omega_{\text{int}}/\omega_{\text{ext}}$ tends to "lock in" to a rational ratio P/Q . Each locked state is stable over a finite range of ω_{ext} . As the external forcing amplitude A_{ext} increases, each locked region becomes wider, forming "Arnold tongues"¹ in the $(\omega_{\text{ext}}, A_{\text{ext}})$ phase diagram. Between the tongues, the system is quasiperiodic, i.e., the ratio $\omega_{\text{int}}/\omega_{\text{ext}}$ is an irrational number. As the forcing amplitude increases beyond some critical value A_{ext}^c the quasiperiodic states become chaotic. This scenario is called the transition to chaos via quasiperiodicity and has been studied quite intensively in recent years, both theoretically²⁻⁴ and experimentally.^{5,6} Below and at the critical line, very good agreement has been found between experiment and theory based on one-dimensional circle maps.

If, however, the system is kept on a tongue while the forcing amplitude A_{ext} is increased, one observes a multitude of periodic states together with infinite cascades of period doubling. Also, in some places other tongues overlap the given tongue, leading to hysteresis effects. In this Rapid Communication we describe experimental results from a forced Rayleigh-Bénard system, examine the structure of a specific tongue, with $\omega_{\text{int}}/\omega_{\text{ext}} = \frac{8}{13}$ [a rational approximation to the golden mean $(\sqrt{5}-1)/2$], and present a phase diagram of the tongue in the $(\omega_{\text{ext}}, A_{\text{ext}})$ plane. We also study the attractor obtained at an accumulation point of one of the period-doubling sequences we observe in the tongue. In particular, we examine the variation of the density of points in the experimentally obtained attractor and compare this variation to theoretical calculations for models which also period double on their route to chaos. A universal $f(\alpha)$ spectrum of scaling indices characterizes this variation,^{7,8} which we accordingly verify experimentally. A similar comparison between theory and experimental data has recently been performed for the attractor obtained from the same Rayleigh-Bénard system at the onset of chaos via quasiperiodicity.⁹

The experimental system has been described earlier.⁶ It

consists of a small aspect ratio Rayleigh-Bénard cell of size $0.7 \times 0.7 \times 1.4 \text{ cm}^3$ with mercury as the working fluid. In the convective state two rolls are present. For a sufficiently large temperature difference across the cell, the convective rolls become unstable to an oscillatory instability transverse to the rolls which produces temperature fluctuations with a well defined frequency ω_{int} . This frequency is of the order of 0.230 Hz. The external frequency is injected into the system by applying a magnetic field parallel to the roll axis and passing a vertical ac-current sheet asymmetrically through the mercury at the center of the cell. Increasing the forcing current A_{ext} increases the nonlinear coupling between the two oscillators. The stability of the system is typically 10^{-6} /hour, which enables us to study the various resonance phenomena in detail.

In the experiment we measure the temperature T of the fluid at a fixed point on the bottom of the cell. We record both continuous time series and "Poincaré sections," which are discrete time series taken at the external forcing frequency ω_{ext} . We extract the periodicities of the system using fast Fourier transforms on the continuous series and autocorrelations on the discrete series. Short system periods may be determined by eye by displaying the Poincaré section as an attractor (by graphing T_t vs $T_{t+1/\omega_{\text{ext}}}$) and counting the number of clumps of points.

During measurements, we keep the forcing amplitude at a constant value and sweep across the tongue, changing the forcing frequency in steps of typical size 0.0002 Hz. We sweep the frequency in both directions to check for hysteresis. In most cases, after a frequency step, the system relaxes to its final state over a period of about 10 min. However, close to boundaries where the $\omega_{\text{int}}/\omega_{\text{ext}}$ state changes, the relaxation time can be much longer.

We now concentrate on the tongue with $\omega_{\text{int}}/\omega_{\text{ext}} = \frac{8}{13}$. Figure 1 shows the tongue in the $(\omega_{\text{ext}}, A_{\text{ext}})$ plane. The curves on the tongue are the borderlines where the periodicity of the signal changes. Each region is labeled by a number n which indicates a periodic state with $\omega_{\text{int}}/\omega_{\text{ext}} = n \cdot 8/n \cdot 13$. In such a region the temperature time series is periodic with period $\tau_n = 13n/\omega_{\text{ext}}$. As we increase the forcing amplitude, we first observe a smooth transition (in-

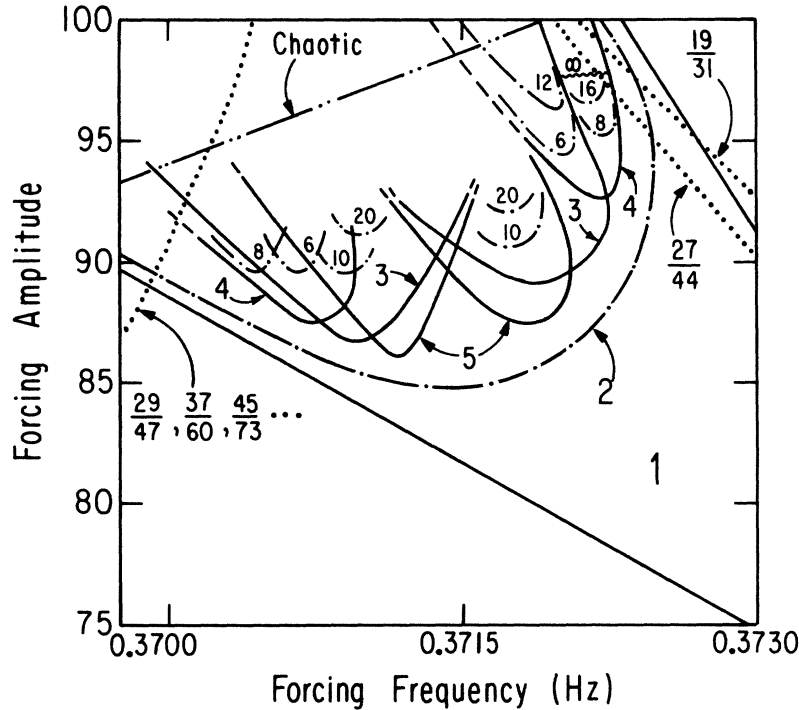


FIG. 1. The tongue with $P/Q = \frac{8}{13}$ shown in the A_{ext} vs ω_{ext} plane. The lines on the tongue refer to transitions between different periodic states. The areas labeled by n correspond to $n \cdot 8/n \cdot 13$ states. The single dotted lines indicate smooth period-doubling transitions. The solid lines indicate discontinuous or symmetry-breaking transitions. The dotted lines on the right- and left-hand sides of the tongue indicate the position of overlapping tongues. The double dotted line indicates the region where the system is chaotic for all forcing frequencies.

indicated by a single dotted line) to a period-doubled state. The boundary of this period doubling is a continuous line stretching across the tongue. It bends smoothly upwards and converges asymptotically to the tongue edge for large forcing amplitudes. Above this line the system does not double its period to a $n=4$ state for all forcing frequencies. Instead, we observe a symmetry breaking into paired regions of fixed multiplicities (indicated by solid lines). Proceeding from the center of the tongue, we find, in order, subregions with multiplicity 5, 3, and 4. These subregions overlap as shown. Overlaps are generally bistable. Each of these subregions contains a period-doubling cascade (indicated by single dotted lines) of period $n \times 2^m$ states. The period 4 cascade on the right-hand side (high forcing frequency) is stable over the largest frequency range. The approximate boundary of the 2^∞ cycle for this cascade is indicated by a wavy line. In addition, there appear to be two regions of $n=7$ which are too small to resolve and are not indicated. The boundaries of all these subregions appear to be smooth. For very strong forcing the system is chaotic at all frequencies as indicated by the double dotted line. We are not able to resolve the structure of the central region of the tongue which contains very long period, intermittent, and chaotic states. The overall structure is different from that expected from one-dimensional circle maps where the $n=2$ state can only produce $n=4$ states and the border of the $n=4$ regions exhibits a cusp.^{10,11} We emphasize that the circle map does yield the correct scaling of tongue widths and positions for

all tongues below and at the critical line.⁶

For large forcing amplitudes we find that neighboring tongues overlap the $\frac{8}{13}$ tongue as predicted by the circle map model.⁴ On the right side of the tongue (high forcing frequency), we find the states with $P/Q = (n \cdot 3 + m \cdot 8) / (n \cdot 5 + m \cdot 13)$, generated by Farey sums with the tongue $\frac{3}{5}$ (e.g., $P/Q = \frac{19}{31}, \frac{27}{44}, \dots$). We find similar high denominator states overlapping the left side of the tongue (low forcing frequency) with $P/Q = (n \cdot 21 + m \cdot 8) / (n \cdot 34 + m \cdot 13)$, generated by Farey sums with the tongue $\frac{21}{34}$. The dotted lines indicate the edges of the regions of overlap of these higher-order tongues. Where either tongues or subregions overlap we observe multistability and hysteresis, with many possible final states for the same values of the system parameters.

Due to long term frequency drift, the very detailed structure of the tongue is hard to observe experimentally, but we suspect that there exist many tiny regions with very high values of n . We are in the process of investigating this surprisingly complex structure in more detail, and plan a study of transients in the tongue. Also, we are studying the structure of other tongues. These results will be reported elsewhere.¹² One preliminary result of interest is that the $\frac{5}{8}$ tongue is qualitatively like the $\frac{8}{13}$ tongue.

We have also studied the structure of the attractor obtained at the accumulation point of the 4×2^m period-doubling cascade which appears at the right side of the tongue. We are able to identify four doublings. However, we cannot resolve the region between the fourth doubling

and the chaotic state. The attractors for the pure $\frac{8}{13}$ state and for the $8 \cdot 8/8 \cdot 13$ state are shown in Fig. 2. Up to five bifurcations have been observed previously in the same Rayleigh-Bénard system without external forcing.¹³

Recently, it was shown that the variation in the density of points on the attractor is conveniently described by a continuous spectrum of scaling indices $f(\alpha)$ and that this spectrum is universal for numerically calculated period-doubling attractors.^{7,8} If the density of points within a distance l around a point x_i is denoted $p_i(l)$, the corresponding scaling index (or singularity¹⁴) is defined as

$$p_i(l) = l^{\alpha_i(l)} \quad (1)$$

Theoretically it is found that the α_i 's fall in an interval $[\alpha_{\min}, \alpha_{\max}]$ where both α_{\min} and α_{\max} are determined by Feigenbaum's¹⁵ universal scaling number $\alpha_{pd} = -2.502907876 \dots$. The other ingredient of the formalism is the index $f(\alpha)$, which is the dimension of the set of points on the attractor which possess the same value of the scaling index α .^{7,14,16} Clearly, $0 \leq f(\alpha) \leq D_0$, where $D_0 = 0.5380451435 \dots$ is the dimension of the attractor.⁸

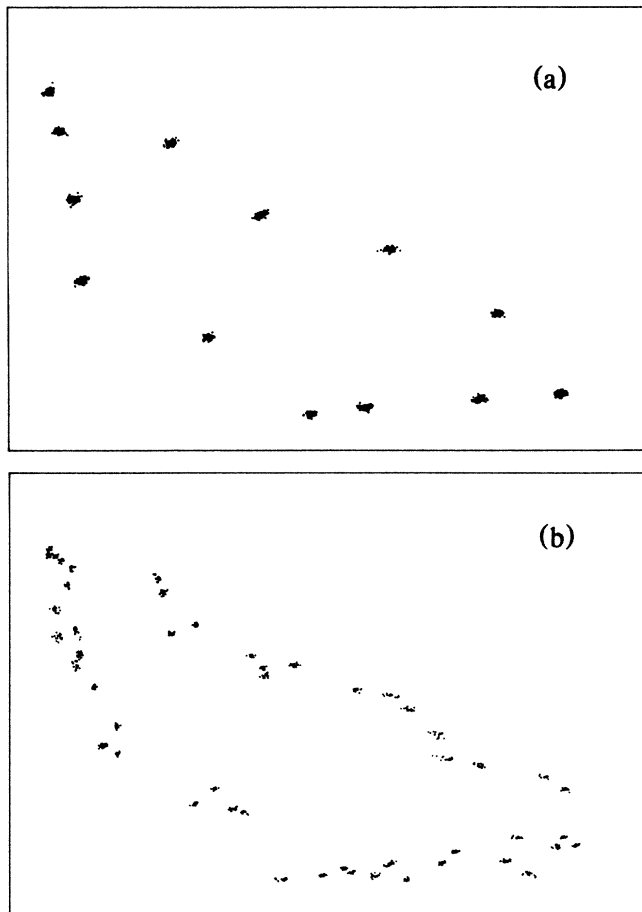


FIG. 2. Attractors obtained at the cascade at the right-hand side of the tongue. The points are found by strobing the temperature signal from the bolometer on the bottom of the cell at the frequency of the external forcing. (a) Pure $\frac{8}{13}$ state. (b) $8 \cdot 8/8 \cdot 13$ state.

For more detailed information about the formalism, see Ref. 7.

This definition (1) does not allow us to obtain results directly from the noisy experimental signal. Instead, we use an averaging trick which has proved very successful in treating experimental data on the transition to chaos via quasiperiodicity.⁹ For a given point in the Poincaré section x_i we follow the time series in steps of the basic period $Q = 13$, until we return to x_i within a distance l (it is important to consider the points modulo $Q = 13$ which assures that we work within a bifurcated "island"). We call the number of steps taken the "recurrence time"⁹ and denote it $m_i(l)$. If the density $p_i(l)$ is very high, we expect the recurrence time to be short. On the other hand, if $p_i(l)$ is small, we expect the recurrence time to be large. We thus assume,⁹

$$p_i(l) \sim [m_i(l)]^{-1} \quad (2)$$

In the scaling analysis we consider different moments of p_i in order to change the importance of various densities. To assure good statistics, we wish to average over all points on the attractor. We therefore calculate a "partition function"

$$\Gamma(q, l) = \langle p_i(l)^{q-1} \rangle \sim \langle m_i(l)^{1-q} \rangle, \quad (3)$$

where the brackets stand for averaging over all points. As $l \rightarrow 0$, we expect to find $\Gamma(q, l) \sim l^{\tau(q)}$. We then translate the function $\tau(q)$ into the $f(\alpha)$ spectrum using the relations^{7,16}

$$\alpha(q) = d\tau(q)/dq, \quad (4)$$

$$f(q) = qd\tau/dq - \tau(q).$$

Plotting $\ln\Gamma(q, l)$ vs $\ln l$ we read off $\tau(q)$ using a straight-line fit. For a period-doubling attractor obtained numeri-

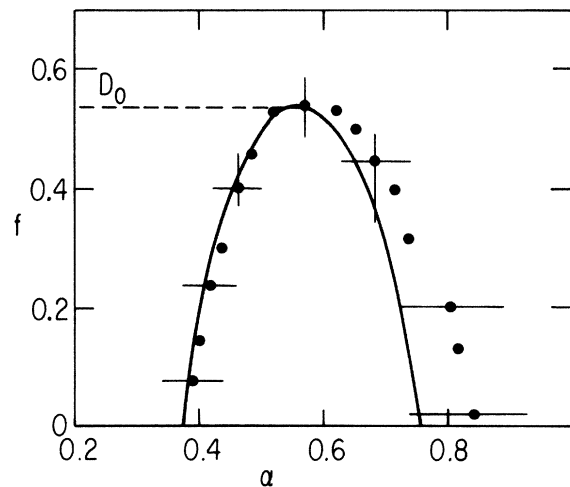


FIG. 3. The $f(\alpha)$ spectrum calculated for a period-doubling attractor at the onset of chaos is shown by the curve (Ref. 7). The corresponding experimental estimates found for the period-doubling attractor at the right side of the tongue are shown by the dots. The error bars are estimated by varying the interval in l over which straight lines were fitted.

cally by iterating maps at the accumulation point, we obtain the curve shown in Fig. 3.⁷ We have also calculated this curve using an exact renormalization group method.⁸ When possible, we fit the data over two decades in the scale l to obtain the results shown by the dots in Fig. 3. In our calculations on the experimental data we choose the fitting interval in l to obtain the best scaling. We estimate the errors by considering how the calculated slope varies with the fitting range. The error is least ($\sim 6\text{--}8\%$) at the left-most part of the curve (which corresponds to positive q). The error at the top point is around $10\text{--}12\%$ and the error at the lower right-hand part (corresponding to large negative q values) is around 20% . The experiment agrees with the theory within this error.

We conclude that the scaling of the experimental attractor at the onset of chaos via period doubling is identical to that of the theoretical attractor obtained at the critical

point, and that we have experimentally verified the universal scaling number $\alpha_{pd} = -2.5029\dots$ to within $6\text{--}8\%$ and the dimension of the set $D_0 = 0.5380\dots$ to within $10\text{--}12\%$. To conclude our study of the tongue, it appears that the experimentally determined structure is similar but not identical to that predicted by the one-dimensional circle map. We suspect that a simple two-dimensional extension of the map should suffice to describe our results and we urge further theoretical calculations along these lines.

We are grateful to L. Kadanoff, I. Procaccia, and C. Tresser for discussions. This work has been supported by the National Science Foundation through Grant No. DMR 83-16204. One of us (M.H.J.) acknowledges support from the Materials Research Laboratory at the University of Chicago.

¹V. I. Arnold, *Trans. Am. Math. Soc., Ser. 2* **46**, 213 (1965); see also, M. R. Herman, in *Geometry and Topology*, edited by J. Palis (Springer, Berlin, 1977), Vol. 597, p. 271.

²Scott J. Shenker, *Physica D* **5**, 405 (1982).

³M. J. Feigenbaum, L. P. Kadanoff, and Scott J. Shenker, *Physica D* **5**, 370 (1982); S. Ostlund, D. Rand, J. P. Sethna, and E. D. Siggia, *Phys. Rev. Lett.* **49**, 132 (1982); *Physica D* **8**, 303 (1983).

⁴M. H. Jensen, P. Bak, and T. Bohr, *Phys. Rev. Lett.* **50**, 1637 (1983); *Phys. Rev. A* **30**, 1960 (1984); P. Cvitanović, M. H. Jensen, L. P. Kadanoff, and I. Procaccia, *Phys. Rev. Lett.* **55**, 343 (1985).

⁵A. P. Fein, M. S. Heutmaker, and J. P. Gollub, *Phys. Scr. T* **9**, 79 (1985).

⁶J. Stavans, F. Heslot, and A. Libchaber, *Phys. Rev. Lett.* **55**, 596 (1985).

⁷T. C. Halsey, M. H. Jensen, L. P. Kadanoff, I. Procaccia, and B. I. Shraiman, *Phys. Rev. A* **33**, 1141 (1986).

⁸D. Bensimon, M. H. Jensen, and L. P. Kadanoff, *Phys. Rev. A* **33**, 3622 (1986).

⁹M. H. Jensen, L. P. Kadanoff, A. Libchaber, I. Procaccia, and J. Stavans, *Phys. Rev. Lett.* **55**, 2798 (1985).

¹⁰L. Glass and R. Perez, *Phys. Rev. Lett.* **48**, 1772 (1982); *Phys. Lett.* **90A**, 441 (1982).

¹¹S. Fraser and R. Kapral, *Phys. Rev. A* **30**, 1017 (1984); see also, D. G. Aronson, M. A. Chory, G. R. Hall, and P. R. McGehee, *Commun. Math. Phys.* **83**, 303 (1982); R. S. MacKay and C. Tresser (unpublished).

¹²J. A. Glazier, A. Libchaber, and J. Stavans (unpublished).

¹³A. Libchaber, C. Laroche, and S. Fauve, *Physica D* **7**, 73 (1983); *J. Phys. (Paris) Lett.* **43**, L211 (1982).

¹⁴T. C. Halsey, P. Meakin, and I. Procaccia, *Phys. Rev. Lett.* **56**, 854 (1986).

¹⁵M. J. Feigenbaum, *J. Stat. Phys.* **19**, 25 (1978); **21**, 669 (1979).

¹⁶U. Frisch and G. Parisi, in *Turbulence and Predictability in Geophysical Fluid Dynamics and Climate Dynamics, Proceedings of the Enrico Fermi International School of Physics, Course LXXXVIII*, edited by M. Ghil, R. Benzi, and G. Parisi (North-Holland, New York, 1985), p. 84.